ISSN 0023-1584, Kinetics and Catalysis, 2010, Vol. 51, No. 4, pp. 529–533. © Pleiades Publishing, Ltd., 2010.

Synthesis and Characterization of TiO_2–Montmorillonite Nanocomposites and Their Photocatalytic Activity[1]

Aiqin Zhang[a,c], Rongbin Zhang[a,*], Ning Zhang[a], Sanguo Hong[a], and Ming Zhang[b]

[a] *Department of Chemistry, Nanchang University, China*

[b] *College of Chemistry, Jiangxi Normal University, Nanchang, Jiangxi, China*

[c] *College of Environmental and Chemical Engineering, Nanchang Hangkong University, Jiangxi, China*

**e-mail: rbzhang@ncu.edu.cn*

Received May 2, 2009

Abstract—TiO_2 nanoparticles have been synthesized on the surface of exfoliated montmorillonite at a low temperature in benzyl alcohol medium. According to X-ray diffraction (XRD), N_2 adsorption-desorption isotherm and transmisson electron microscopy (TEM), it was found that the intercalation of TiO_2 nanoparticles destroyed the ordered structure of montmorillonite to some extent, and the crystallites of the nanocomposites are assembled to form a house-of-cards structure. The size of the nanoparticles in the interlamellar space is about 4 nm. The nanocomposites exhibited excellent photocatalytic activity in methylene blue degradation due to the synergetic effect of the adsorptive ability to organic compound of cetyl trimethylammonium bromide—montmorillonite and the catalytic ability of TiO_2 nanoparticles in it.

DOI: 10.1134/S0023158410040117

INTRODUCTION

Montmorillonite (**MMT**) is a layered aluminosilicate of 2:1 type structure: one octahedral layer takes place between two tetrahedral layers, resulting in weak van der Waals interaction between the adjacent lamellae (Si–O···Si). This structure causes MMT to be easily disaggregated, and it has a high cationic exchange capacity ensuring favorable conditions for intercalation reactions. Up to date, MMT has been found many applications in heterogeneous catalysis as catalyst support [1–3]. It has been reported that metal oxides nanoparticles have been deposited on MMT with some nanoparticles intercalated into its interlayers. These MMT-based catalysts combines the functions of the nanoparticles and MMT together, and exhibited synergetic effects [4–6]. Now several transition metal oxide-pillared clay systems, such as TiO_2 [7], ZnO [8], Fe_2O_3 [9], ZrO_2 [10], and CoO on SiO_2-aluminosilicate [11], have been reported. Generally, most of these pillared clays are prepared by exchanging charge-compensating cations between the clay layers with larger inorganic hydroxyl cations, which are polymeric or oligomeric hydroxyl metal cations formed by the hydrolysis of metal salts. The calcination process is usually necessary to yield metal oxide "pillars." This article introduces a novel one-step route for the synthesis of TiO_2–MMT nanohybrid. The simple approach involves the in situ growing of TiO_2 nanoparticles with anatase phase immobilized on the exfoliated MMT at low temperature.

[1] The article is published in the original.

EXPERIMENTAL

Preparation of the Nanocomposites

$TiCl_4$, NaCl, **CTAB** (cetyl trimethylammonium bromide) were analytical grade and were used without further purification. The chemical formula of the Ca–MMT can be expressed as $Ca_{0.19}Mg_{0.06}Na_{0.01} \cdot (Si_{3.96}Al_{0.04})(Al_{1.44}Fe_{0.09}Mg_{0.47})O_{10}(OH)_2 \cdot nH_2O$. The cation-exchange capacity of the clay was 66.5 mmol/100 g.

The Ca–MMT was subjected to cation exchange reaction to replace the interlayer ion with a cationic surfactant, cetyl trimethylammonium (**CTA**). After ion exchange reaction, excess surfactants were thoroughly removed by washing with hot distilled water and then dried under an ambient atmosphere. The CTA-exchanged MMT (**CTAB-MMT**) dispersed in benzyl alcohol under stirring to obtain 1 wt %colloidal suspension of delaminated clay particles. A certain amount of $TiCl_4$ was slowly added to anhydrous benzyl alcohol (benzyl alcohol : $TiCl_4$ = 20 : 1, v/v) under vigorous stirring at room temperature to obtain a solution. The colloidal suspension and the solution of $TiCl_4$ obtained above were mixed to reach a Ti : MMT ratio of 10 mmol/g, stirred for 30 min and kept at 50 or 70°C for 24 h. The suspension was separated by centrifuging and precipitate was washed with ethanol and THF and dried at room temperature. All the samples obtained were milled into powder and marked as

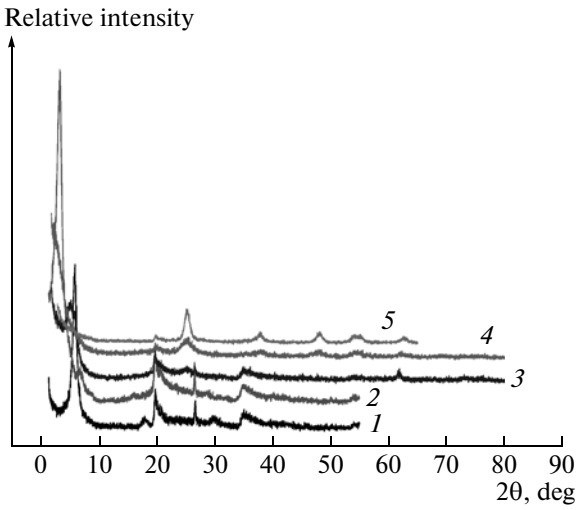

Fig. 1. XRD patterns of nanocomposites and MMT: *1*—pristine MMT, *2*—CTAB–MMT, *3*—TiO_2–CTAB–MMT-50, *4*—TiO_2–CTAB–MMT-70, *5*—TiO_2–MMT-70 calcinated at 450°C.

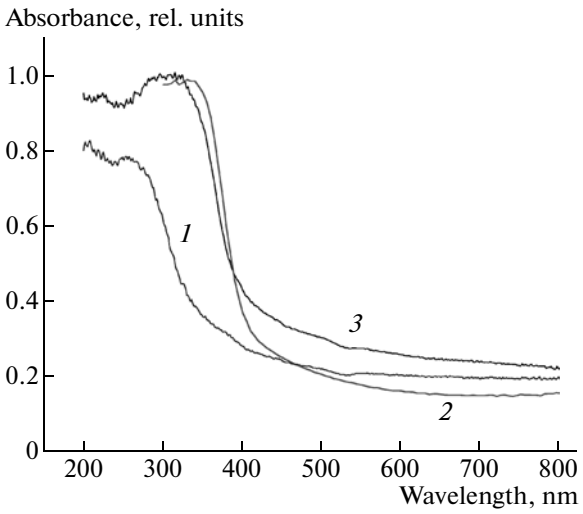

Fig. 2. UV-Vis absorption spectra: *1*—Ca–MMT, *2*—TiO_2, *3*—TiO_2–MMT-70.

TiO_2–CTAB–MMT-50 and TiO_2–CTAB–MMT-70 respectively. The pure TiO_2 was also prepared by the same method at 70°C without adding of the colloidal suspension of delaminated clay particles.

Characterization

The crystallinity of the samples was evaluated by powder X-ray diffraction (**XRD**) on an X-ray diffractometer (Bruker D8 Advance) with CuK_α radiation under operation conditions of 40 kV and 40 mA in the 2θ range from 1.5° to 80°. Transmission electron microscopy (**TEM**) images were taken using JEM-2010(HR). The absorption edge of the samples was measured using a UV-Vis spectrophotometer (U-3310) and $BaSO_4$ was the reflectance standard in a UV-Vis diffuse reflectance experiments. Surface areas and porosities were determined from the adsorption-desorption isotherms of N_2 at 77 K after degassing the samples at 393 K with a Micromeritics ASAP 2020 apparatus.

Photocatalytic Activity Measurement

The reactor was illuminated by a high pressure Hg lamps (500 W) which predominantly emit light at 365 nm. In a typical reaction, sample of TiO_2–MMT-70 nanohybrid (50 mg) or TiO_2 (16 mg) was first immersed in an aqueous methylene blue (**MB**) solution (20 mg/l, 100 ml) in the dark for 24 h to establish the adsorption equilibrium, then centrifuged and immersed in another MB solution (20 mg/l, 50 ml). The photocatalytic activities of the samples were assessed by monitoring the adsorbance of MB at 660 nm at given irradiation time intervals.

RESULTS AND DISCUSSION

XRD Patterns

The powder XRD patterns of pristine MMT, CTAB–MMT and TiO_2–MMT nanocomposites are shown in Fig. 1. The XRD patterns of MMT generally show basal 001 reflection and two dimensional diffraction *hk* only, and other *hkl* diffractions are usually not observed [12]. TiO_2–CTAB–MMT-70 nanocomposite do not exhibit 001 reflection, indicating the delamination of the aluminosilicate layers [13]. The peak at 25.3° in all nanocomposites is the (101) plane of the anatase phase of titania. No rutile phase of titania was found in the samples. The peak at 25.3° became more intense and sharper after TiO_2–CTAB–MMT-70 was calcined at 450°C for 2 h, but the peak is still relatively broad due to the nanosized TiO_2 particles. It revealed that the presence of MMT hindered the agglomeration of the TiO_2 nanoparticles.

UV-Vis Diffuse Reflectance Spectra

Figure 2 illustrates UV-Vis spectra for the TiO_2–MMT-70, in comparison with those for MMT and TiO_2. Pure MMT was almost transparent in the wavelength range longer than 350 nm [14], the absorption edge of the nanocomposite has a blue-shift in comparison to that of pure TiO_2. Some authors [15, 16] have also reported that the absorption edge of TiO_2-mont-

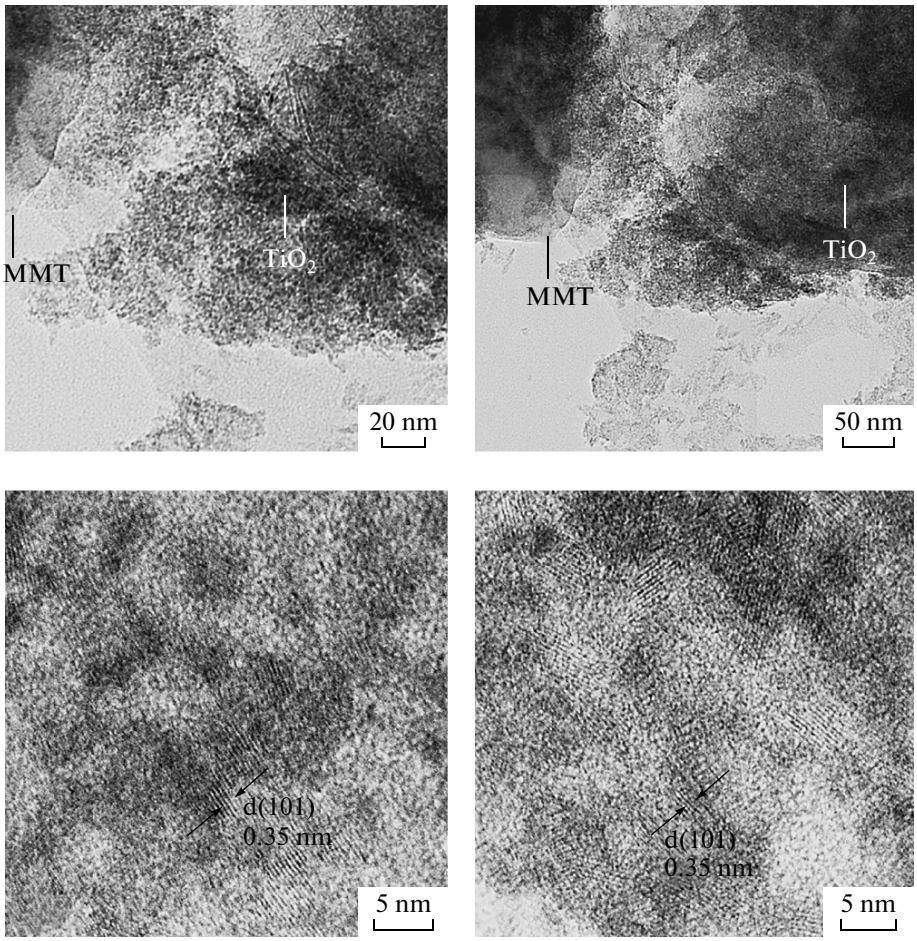

Fig. 3. TEM images of TiO_2–MMT-70.

morillonite nanocomposite had a blue-shift that was due to quantum size effects arising from TiO_2.

Transmission Electron Microscopy

According to TEM micrographs in Fig. 3, the nanohybrid exhibited two distinct images, sheets and spherical particles. The former are the exfoliated sheets of montmorillonite whereas the latter are the TiO_2 nanoparticles. The mean size of spherical particles is around 4 nm estimated from the scale bar, which is in good agreement with that calculated from XRD peak broadening according to Scherrer equation. In Fig. 3, two HR–TEM images were also presented. They clearly showed that the lattice fringe spacing corresponding to the (101) planes of the anatase phase is about 0.35 nm.

N_2 Adsorption–Desorption

Figure 4 showed the adsorption-desorption isotherms of nitrogen for pristine MMT, TiO_2–MMT-70,

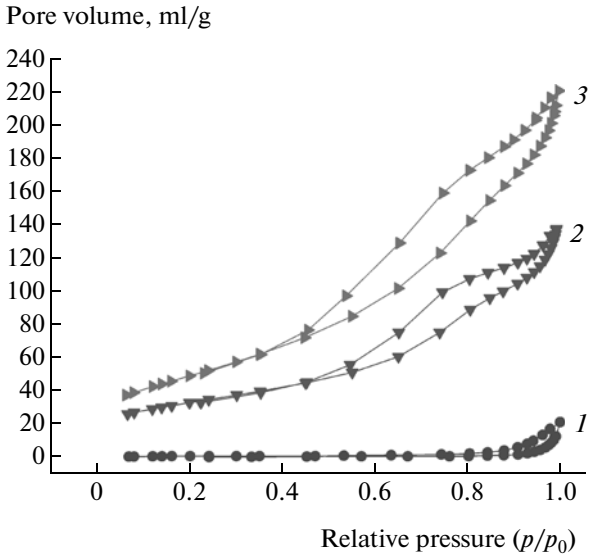

Fig. 4. N_2 adsorption-desorption isotherms: *1*—pristine MMT, *2*—TiO_2–CTAB–MMT-70, *3*—TiO_2–CTAB–MMT-70 calcinated at 450°C.

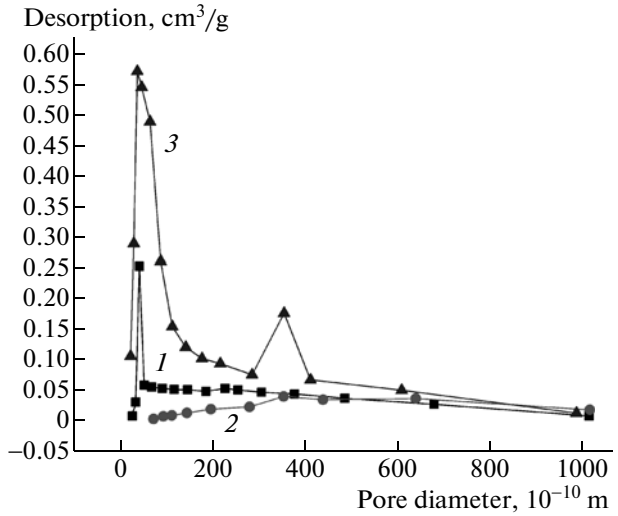

Fig. 5. Pore size distribution in samples: *1*—pristine MMT, *2*—TiO_2–CTAB–MMT-70, *3*—TiO_2–CTAB–MMT-70 calcinated at 450°C.

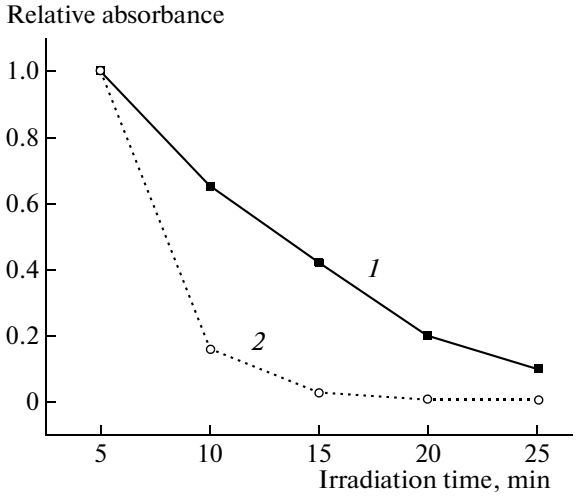

Fig. 6. Degradation of methylene blue on commercial TiO_2 (*1*) and TiO_2–CTAB–MMT-70 (*2*).

and TiO_2–MMT-70 calcinated at 450°C. All these isotherms can be classified as the BDDT-type IV shape, implying bimodal pore size distributions in the mesoporous and macroporous regions. The nitrogen uptakes of the TiO_2–MMT-70 was substantially lower, compared with that of the pristine MMT. The small hysteresis of the nanocomposite indicated less mesoporosity. But the nitrogen uptakes of the nanocomposite increased after it was calcinated at 450°C for 2 h, implying that the elimination of the organic moiety giving rise to mesopores in the interlayers. According to adsorption data, the specific surface area is reduced from 80 m^2/g for the pristine MMT to 10 m^2/g for the TiO_2–MMT-70 due to the modification of CTAB and TiO_2 nanoparticles and enlarged to 180 m^2/g for TiO_2–MMT after calcination. The bimodal size distributions were further confirmed by the corresponding pore size distribution curves in Fig. 5.

Photocatalytic Activity

According to elemental analysis, the mass content of TiO_2 in TiO_2–CTAB–MMT-70 was 33.5%, so the weight of TiO_2 in nanocomposite was the same as commercial TiO_2 powder in photocatalytic test. As shown in Fig. 6, it was easily found that TiO_2–CTAB–MMT-70 exhibited higher photocatalytic activity toward MB degradation than TiO_2 powder. This may be due to a combination of the adsorptive ability of organic MMT and the catalytic ability of TiO_2 nanoparticles in it.

So TiO_2 nanoparticles have been synthesized on the surface of MMT at a low temperature in benzyl alcohol medium. According to XRD, N_2 adsorption-desorption isotherms and TEM, it was found that the intercalation of TiO_2 nanoparticles destroyed the ordered structure of MMT to some extent, and the crystallites of the nanohybrids were assembled to form a house-of-cards structure. The size of the nanoparticles in the interlamellar space was in about 4 nm according to XRD patterns and TEM. The nanocomposite exhibited excellent photocatalytic activity toward MB degradation due to the synergetic effect of the adsorptive ability to organic compound of CTAB–MMT and the catalytic ability of TiO_2 nanoparticles in it.

ACKNOWLEDGMENTS

This work was financially supported by program of National Natural Science Foundation of China (20763005/B030301).

REFERENCES

1. Okada, T., Watanabea, Y., and Ogawa, M., *Chem. Commun.*, 2004, vol. 3, p. 320.
2. Király, Z., Veisz, B., Dékány, I., Mastalir, Á., and Rázga, Z., *Chem. Commun.*, 1999, vol. 19, p. 1925.
3. Ishii, R., Wada, H., and Ooi, K., *Chem. Commun.*, 1998, vol. 16, p. 1705.
4. Dékány, I., Túri, L., Galbács, G., and Fendle, J.H., *J. Colloid Interface Sci.*, 1999, vol. 213, p. 584.
5. Miyoshi, H., Mori, H., and Yoneyama, H., *Langmuir*, 1991, vol. 7, p. 503.
6. Ogawa, M., Ishii, T., Iyamoto, N., and Kuroda, K., *Adv. Mater.*, 2001, vol. 13, p. 1107.
7. Sterte, J.P., *Clays Clay Miner.*, 1986, vol. 34, p. 658.
8. Hur, S.G., Kim, T.W., Hwang, S.-J., Yang, J.H., and Choy, J.-H., *J. Phys. Chem. B,* 2006, vol. 110, p. 1599.

9. Burch, R. and Warburton, C.I., *Appl. Catal.*, 1987, vol. 33, p. 395.

10. Bartley, G.J.J. and Burch, R., *Appl. Catal.*, 1985, vol. 19, p. 175.

11. Choy, J.H., Jung, H., Han, Y.S., Yoon, J.B., Shul, Y.G., and Kim, H., *Chem. Mater.*, 2002, vol. 14, p. 3823.

12. Long, R.Q. and Yang, R.T., *J. Catal.*, 1999, vol. 186, p. 254.

13. Miao, S.D., Liu, Z.M., Han, B.X., Zhang, J.L., Yu, X., Du, J.M., and Sun, Z.Y., *J. Mater. Chem.*, 2006, vol. 16, p. 579.

14. Ooka, C., Yoshida, H., Suzuki, K., and Hattori, T., *Microporous Mesoporous Mater.*, 2004, vol. 67, p. 143.

15. Miao, S.D., Liu, Z.M., Han, B.X., Zhang, J.L., Yu, X., Du, J.M., and Sun, Z.Y., *J. Mater. Chem.*, 2006, vol. 16, p. 579.

16. Ooka, C., Yoshida, H., Horio, M., Suzuki, K., and Hattori, T., *Appl. Catal., B*, 2003, vol. 41, p. 313.